



HAL
open science

Controlling Anthropogenic and Natural Seismicity: Insights From Active Stabilization of the Spring-Slider Model

Ioannis Stefanou

► **To cite this version:**

Ioannis Stefanou. Controlling Anthropogenic and Natural Seismicity: Insights From Active Stabilization of the Spring-Slider Model. *Journal of Geophysical Research: Solid Earth*, 2019, 124 (8), pp.8786-8802. 10.1029/2019JB017847 . hal-02469049

HAL Id: hal-02469049

<https://hal.science/hal-02469049>

Submitted on 6 Feb 2020

HAL is a multi-disciplinary open access archive for the deposit and dissemination of scientific research documents, whether they are published or not. The documents may come from teaching and research institutions in France or abroad, or from public or private research centers.

L'archive ouverte pluridisciplinaire **HAL**, est destinée au dépôt et à la diffusion de documents scientifiques de niveau recherche, publiés ou non, émanant des établissements d'enseignement et de recherche français ou étrangers, des laboratoires publics ou privés.

15 **Abstract**

16 We present a theoretical study focusing on exploring the possibility of controlling an-
 17 thropogenic and natural seismicity. We actively control the pressure of injected fluids
 18 using a negative-feedback control system. Our analysis is based on the spring-slider model
 19 for modeling the earthquake instability. We use a general Coulomb-type rheology for de-
 20 scribing the frictional behavior of a fault system. This model leads to a non-autonomous
 21 system, whose steady-state and stability are studied using a double-scale asymptotic anal-
 22 ysis. This approach renders the dominant order of the system time invariant. Established
 23 tools from the classical mathematical theory of control are used for designing a proper
 24 stabilizing controller. We show that the system is stabilizable by controlling fluid pres-
 25 sure. This is a central result for industrial operations. A stabilizing controller is then de-
 26 signed and tested. The controller regulates in real-time the applied pressure in order to
 27 assure stability, avoid unwanted seismicity and drive the system from unstable states of
 28 high potential energy, to stable ones of low energy. The controller performs well even in
 29 the absence of complete knowledge of the frictional properties of the system. Finally, we
 30 present two numerical examples (scenarios) and illustrate how anthropogenic and nat-
 31 ural earthquakes could be, in theory, prevented.

32 **1 Introduction**

33 Given the current intense human activity for conventional and unconventional en-
 34 ergy production (e.g. oil and gas), renewable energies (e.g. geothermal) and potential
 35 environmental friendly methods related to climate change (e.g. CO₂ sequestration), avoid-
 36 ing anthropogenic seismicity is a challenging topic. Even though evidence and proof of
 37 the origin of reported seismicity and its relation with human activities will always have
 38 a degree of uncertainty, it is nowadays generally accepted that humans can induce or trig-
 39 ger earthquakes. Anthropogenic earthquakes are usually of small to moderate magni-
 40 tude, i.e. less than $M_w = 4$ (moment magnitude). However, they usually exceed the
 41 acceptable limits set by the authorities and can cause damage. Moreover, there are sev-
 42 eral cases where induced earthquakes had important magnitudes (no distinction is made
 43 here between triggered and induced earthquakes and both terms are used interchange-
 44 ably for simplicity). Some examples of induced earthquakes, among several others, are
 45 the $M_w = 5.3$ at Trinidad, Colorado earthquake (EQ) in US due to wastewater injec-
 46 tion (Rubinstein & Mahani, 2015), the $M_w = 5.7$ at Prague, Oklahoma EQ in US prob-

ably due to wastewater injection (Keranen, Savage, Abers, & Cochran, 2013; McGarr, 2014) and the $M_w = 3.6$ at Basel geothermal project in Switzerland (Cornet, 2016; Deichmann & Giardini, 2009). In fact the number and the importance of induced seismicity events were such that the United States Geological Survey (USGS) incorporated them in the 2014 United States National Seismic Hazard Model (Petersen et al., 2015).

Here we address the general question of earthquake control: Is it possible to control and avoid anthropogenic and natural earthquakes and how? We address this question using a mathematically rigorous framework and keeping complexity to a minimum degree. In particular, we investigate the conditions under which a simplified, seismogenic fault system can be stabilized by automatic fluid pressure adjustment/control. The concept that pore pressure increase due to fluid injection can stimulate fault slip is well established, nowadays (Frohlich, 2012; Healy, Rubey, Griggs, & Raleigh, 1968; Hubbert & Rubey, 1959; Raleigh, Healy, & Bredehoeft, 1976). However, the question of EQ control and EQ risk mitigation is still open and challenging.

Evidence of EQ control from field experiments is very limited. We refer to the seminal field experiment of Raleigh et al. (1976) in the 70's in Rangely, Colorado, US, where earthquakes could be turned off and on by varying the pore pressure. Another example of EQ control is in Dale, New York, US (Fletcher & Sykes, 1977), where earthquakes of magnitude -1 to 1.4 formed a cluster about 650m across near the bottom of a 426m injection well. The earthquake activity was arrested when the top hole pressure dropped below 5 MPa. More recent field experiments involve the well monitored tests by Cappa, Scuderi, Collettini, Guglielmi, and Avouac (2019); Guglielmi, Cappa, Avouac, Henry, and Elsworth (2015) performed at 252m depth within the LSBB underground laboratory in France. In these field experiments aseismic slip was systematically preceding seismic slip, giving concrete evidence that slip can be also aseismic.

Here we follow a theoretical approach in order to get useful insight of the controllability of a fault system and the possibility of injecting fluids in a way that guarantees aseismic slip (definitions of the terms seismic and aseismic slip, as used here, are given in Section 2.2). Our analysis is based on the classical spring-slider model. We adopt a general frictional law that depends on slip and rate of slip. Additionally to rock elasticity (spring) we consider also radiational damping. This is performed by accounting for the rock viscosity through a damper in Kelvin-Voigt configuration (see also Wang (2017)).

79 We consider that the rock is saturated and that our system is well oriented for slip in
 80 the ambient stress-field. Both physics and geometry of the system are kept as simple as
 81 possible. The role of heterogeneities, of pore fluid diffusivity and special hydrological con-
 82 ditions are not considered in the present work. Consequently, we don't focus on EQ rup-
 83 ture and propagation in details, but only on average (over the fault's length) using the
 84 spring-slider model. The above mentioned aspects, as well as the observability of the real
 85 system and other techno-economical aspects of EQ control, exceed the scope of the present
 86 article and they are explored in the frame of the ongoing ERC project "Controlling earth-
 87 Quakes - CoQuake" (see <http://coquake.com>).

88 We give particular emphasis on the study of the stability of the system which is
 89 constantly driven by the far-field tectonic velocity. The term *stability* is used here only
 90 in the sense of Lyapunov stability (i.e. the system remains close to its equilibrium state
 91 under small perturbations from it; for a rigorous mathematical definition of Lyapunov
 92 stability we refer to (Lyapunov, 1892; Stefanou & Alevizos, 2016)). Due to the far field
 93 tectonic velocity and the general rheology considered for friction, the system is non-autonomous
 94 (i.e. it depends explicitly on time) and the classical methods of Lyapunov stability can-
 95 not be directly applied. For this purpose, we use a double-time scale asymptotic anal-
 96 ysis that a) eliminates the secular terms (i.e. growing, unbounded terms in time), b) pro-
 97 vides the steady-state of the system describing its slow, creep-like motion and c) allows
 98 to derive the (in-)stability conditions, i.e. determine when slow, creep-like slip is pos-
 99 sible and when an earthquake takes place. Based on these results we prove mathemat-
 100 ically that the system is *stabilizable* by fluid pressure control. This is a major result. An
 101 opposite conclusion would mean that EQ control is impossible, implying inevitable risks
 102 for on-going, large-scale industrial applications.

103 Following these mathematical developments and using the *classical mathematical*
 104 *theory of control* we design a *stabilizing controller (compensator)* and we investigate the
 105 conditions for which the controller can stabilize the system, even when complete knowl-
 106 edge on the evolution of the frictional properties of the system is not available. The abil-
 107 ity of the controller to stabilize the system and avoid unwanted seismicity, is then illus-
 108 trated through two scenarios of fluid injection at 5km depth. The first one refers to an
 109 injection project, where an injection under constant pressure rate is planned. It is shown
 110 that the controller automatically stabilizes the system and avoids the anticipated earth-
 111 quake event of $M_w = 3.8$. The second scenario concerns a fault system with higher rup-

112 ture area, able to give earthquakes of $M_w = 5.8$. In this second scenario, we drive the
 113 system from its initial, high energy, unstable state to a new, stable one. This is done by
 114 automatically adjusting the fluid pressure such as to assure a constant slow slip rate. In
 115 this way no seismicity is observed and the earthquake is avoided. Finally, the robustness
 116 of the designed controller to successfully mitigate seismicity is challenged by perturb-
 117 ing the friction properties of the system.

118 The paper is organized as follows. In Section 2 we present the basic modeling as-
 119 sumptions of the spring-slider analog and we study it using double-scale asymptotics in
 120 time. The steady-state motion is approximated by a power series of the orders of the slow
 121 time scale, for which we calculate explicitly the dominant one. The necessary and suf-
 122 ficient conditions for stable and unstable steady-state motion are determined. This asymp-
 123 totic analysis renders the dominant order of the system time invariant and allows us to
 124 study it further in Section 3 using the classical mathematical theory of control. The lin-
 125 earization of the system is investigated in paragraph 3.2 and its stabilizability in para-
 126 graph 3.3. A stabilizing controller is designed in paragraph 3.4. Asymptotic tracking and
 127 robustness of the controller are discussed next. Finally, in Section 4 we present two nu-
 128 merical examples, i.e. the aforementioned scenarios of EQ control.

129 **2 Steady-state and stability conditions for the spring-slider analog**

130 Consider the spring-slider model of Figure 1a. This is the classical paradigm and
 131 starting point for studying the dynamic instability of earthquake nucleation in a math-
 132 ematically simplified manner (see Burridge and Knopoff (1967); Reid (1910)). In this
 133 model, the block represents the mobilized rock mass, m , during an earthquake event. With
 134 the spring, k , we model the elastic deformation of the surrounding to the fault rock. This
 135 allows to account for the progressive elastic energy build-up due to the far field tectonic
 136 movement, δ_∞ . The far field tectonic movement is of the order of some cm's per year,
 137 contrary to the seismic slip that can rise up to one meter per second. The coefficient of
 138 the elastic spring is proportional to the effective shear elastic modulus of the surround-
 139 ing to the fault rocks, G , and inversely proportional to the fault length, L , i.e. $k \propto \frac{G}{L}$.
 140 This scaling is retrieved from elasticity theory (Palmer & Rice, 1973). With effective shear
 141 modulus we mean the apparent/averaged shear modulus over a region that extends at
 142 a distance L in the direction and perpendicular to the fault (see Figure 1b). This region
 143 includes the damaged area that extends from some meters to some kilometers around

144 the fault (Okubo et al., 2019). Additionally, we consider the effective viscosity of the sur-
 145 rounding rock, C . This viscosity is represented through an equivalent dashpot of coef-
 ficient η , connected in a Kelvin–Voigt configuration as shown in Figure 1.

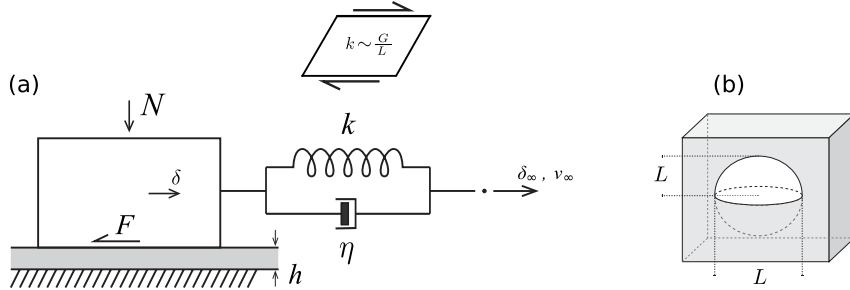


Figure 1. Spring-slider analog.

146

147 With the term *fault* we mean the region of the rock system that is under pronounced
 148 localized shear deformation and opposes to the movement of the block, with a frictional
 149 force F . A fault is usually modeled as a mathematical plane due to its very small thick-
 150 ness, h , compared to the other characteristic lengths of the problem. Nevertheless, its
 151 thickness is linked with the softening response of the system, i.e. the reduction of fric-
 152 tion in function of slip, rate of slip and other variables related to multiphysical couplings.
 153 This region of extreme shearing is usually consisted of ultracataclastic materials and it
 154 has a complex structure (Ben-Zion & Sammis, 2003; Brodie, Fettes, Harte, & Schmid,
 155 2007) due to various physico-chemical phenomena that take place during pre- and co-
 156 seismic slip (see Anthony and Marone (2005); Rattez, Stefanou, and Sulem (2018); Rat-
 157 tez, Stefanou, Sulem, Veveakis, and Poulet (2018a, 2018b); Reches and Lockner (2010);
 158 Scuderi, Colletini, and Marone (2017); Tinti et al. (2016), among others). As a result,
 159 the apparent friction, F , does not depend only on the extent and the rate of slip, δ , $v =$
 160 $\dot{\delta}$, but also on the evolution of the microstructural network, the grain size, the presence
 161 and pressure of interstitial fluids, the temperature, time (state) and the reactivation of
 162 chemical reactions (Brantut and Sulem (2012); Veveakis, Alevizos, and Vardoulakis (2010);
 163 Veveakis, Stefanou, and Sulem (2013), among others).

164

As far as it concerns the triggering of the dynamic instability studied here, the knowl-
 165 edge of the constitutive description of the apparent friction is central. Depending on the
 166 way that the fault's apparent friction evolves with shearing, an earthquake can be nu-

167 cleated or arrested. The transition of the system from a potential unstable state to a sta-
 168 ble one can be studied mathematically.

Let the apparent fault friction depend on δ and $\dot{\delta}$, i.e. $F = F(\delta, \dot{\delta})$. The spring-slider analog is described by the following equation:

$$m\ddot{\delta} = -F_r(\delta, \dot{\delta}) + k(\delta_\infty - \delta) + \eta(v_\infty - v) \quad (1)$$

169 where δ_∞ is the far-field displacement due to the far-field velocity v_∞ . Notice that the
 170 above expression considers the dependence of friction on the degree of freedom of the sys-
 171 tem (slip) and its first derivative (rate of slip) and not on any internal, state variables
 172 (see rate and state friction laws). Nevertheless, it is often possible to eliminate these in-
 173 ternal variables and express friction as a function of slip and rate of slip only. Later, in
 174 paragraph 2.3, the apparent fault friction will depend on the fluid pressure too, which
 175 will allow to control seismic slip.

176 It is worth emphasizing that the above equation is a non-autonomous, non-linear
 177 dynamic system, whose stability and steady state cannot be directly studied using the
 178 classical Lyapunov methods (Brauer & Nohel, 1969). Stability of this system has been
 179 studied in the literature by several researchers who considered it ad-hoc as autonomous
 180 by either neglecting the far field velocity or by applying a constant force. Nevertheless,
 181 this is a strong assumption that can lead, in general, to incorrect results regarding sta-
 182 bility (Brauer & Nohel, 1969). Here we follow a different approach that allows us to asymp-
 183 totically approximate the steady-state movement of the block and study its (Lyapunov)
 184 stability.

185 Due to the fact that the far-field tectonic movement is many orders of magnitude
 186 slower than seismic slip (v_∞ is a very small quantity) the steady-state solution of the spring-
 187 slider can be asymptotically approximated using the double-scale approach presented in
 188 the following paragraph.

189 2.1 Double-scale asymptotic analysis

Equation (1) can be written as follows:

$$\ddot{y} = -a(y, \dot{y}) + c(\varepsilon t - y) + d(\varepsilon - \dot{y}), \quad (2)$$

190 where \ddot{y} and \dot{y} denote, respectively, the second and first order derivatives with respect
 191 to time, t , of the unknown function $y = y(t)$, ε is a small parameter ($\varepsilon \ll 1$) and a ,

192 c, d are of $O(\varepsilon^0)$. The above equation is dimensionless y expresses normalized displacement
 193 and the exact expressions of coefficients are given in Section 4 (Eq.(41)), where the
 194 theory is applied to specific scenarios of earthquake control.

We introduce a new variable $\tau = \varepsilon t$, which defines a long time scale because it is not negligible when τ is of order ε^{-1} or larger. In this way the system is expressed in terms of two time scales, a slow one, τ , and a fast one, t :

$$\ddot{y} = -a(y, \dot{y}) + c(\tau - y) + d(\varepsilon - \dot{y}). \quad (3)$$

This double scale approach allows to seek solutions of y , which are functions of both variables t and τ , treated as independent (Bender & Orszag, 1999). It is worth emphasizing that expressing y as a function of two variables is an artifice to remove secular effects. The exact solution $y(t)$ is a function of t alone. We assume the following perturbation expansion for the unknown function $y(t)$:

$$y(t) = y_0(t, \tau) + \varepsilon y_1(t, \tau) + \varepsilon^2 y_2(t, \tau) + O(\varepsilon^3). \quad (4)$$

Using the chain rule for differentiation, we obtain:

$$\frac{dy(t)}{dt} = \frac{\partial y_0}{\partial t} + \varepsilon \left(\frac{\partial y_0}{\partial \tau} + \frac{\partial y_1}{\partial t} \right) + \varepsilon^2 \left(\frac{\partial y_1}{\partial \tau} + \frac{\partial y_2}{\partial t} \right) + O(\varepsilon^3) \quad (5)$$

and

$$\frac{d^2 y(t)}{dt^2} = \frac{\partial^2 y_0}{\partial t^2} + \varepsilon \left(2 \frac{\partial^2 y_0}{\partial \tau \partial t} + \frac{\partial^2 y_1}{\partial t^2} \right) + \varepsilon^2 \left(\frac{\partial^2 y_0}{\partial \tau^2} + 2 \frac{\partial^2 y_1}{\partial \tau \partial t} + \frac{\partial^2 y_2}{\partial t^2} \right) + O(\varepsilon^3). \quad (6)$$

We assume that $a(y, \dot{y})$ can be expanded in power series in terms of ε :

$$a(y, \dot{y}) = a(y_0, \frac{\partial y_0}{\partial t}) + \varepsilon \left[\frac{\partial a}{\partial y} \Big|_{(y_0, \frac{\partial y_0}{\partial t})} y_1 + \frac{\partial a}{\partial \dot{y}} \Big|_{(y_0, \frac{\partial y_0}{\partial t})} \left(\frac{\partial y_0}{\partial \tau} + \frac{\partial y_1}{\partial t} \right) \right] + O(\varepsilon^3). \quad (7)$$

Inserting the above equations into Eq.(2) and collecting powers of ε , we obtain the following cascade problems:

$$\begin{aligned} \varepsilon^0 : \quad & \frac{\partial^2 y_0}{\partial t^2} = -a(y_0, \frac{\partial y_0}{\partial t}) + c(\tau - y_0) - d \frac{\partial y_0}{\partial t} \\ \varepsilon^1 : \quad & \frac{\partial^2 y_1}{\partial t^2} = - \left(\frac{\partial a}{\partial y} \Big|_{(y_0, \frac{\partial y_0}{\partial t})} + c \right) y_1 - \left(\frac{\partial a}{\partial \dot{y}} \Big|_{(y_0, \frac{\partial y_0}{\partial t})} + d \right) \frac{\partial y_1}{\partial t} - \left(\frac{\partial a}{\partial \dot{y}} \Big|_{(y_0, \frac{\partial y_0}{\partial t})} + d \right) \frac{\partial y_0}{\partial \tau} - 2 \frac{\partial^2 y_0}{\partial t \partial \tau} + d \\ \varepsilon^2 : \quad & \dots \end{aligned} \quad (8)$$

195

2.2 Slow dynamics and Lyapunov stability

We will first study the first of Eqs.(8). Setting $q(t) = \frac{\partial y_0(t, \tau)}{\partial t}$ and $r(t) = y_0(t, \tau)$ we obtain the following first order, non-linear system of ODE's:

$$\begin{aligned}\dot{q} &= -a(r, q) + c(\tau - r) - d q \\ \dot{r} &= q.\end{aligned}\tag{9}$$

Notice that in this system, τ acts as a parameter, given that t and τ are independent variables. The above system can be written in vectorial form $\dot{z} = f(z)$, with $z = (z_1, z_2) = (q, r)$, is autonomous and its stability can be studied using the classical tools of Lyapunov stability theory (see Brauer and Nohel (1969)). This system has an equilibrium point (fixed point) at $z^* = (q^*, r^*)$ satisfying:

$$\begin{aligned}-a(r^*, q^*) + c(\tau - r^*) &= 0 \\ q^* &= 0.\end{aligned}\tag{10}$$

196

197

198

199

The above fixed point shows that the system has zero velocity in terms of the fast time variable t , i.e. $q^* = \frac{\partial y_0^*(t, \tau)}{\partial t} = 0$, leading to $y_0 = y_0(\tau)$, which is a function of the slow time variable, only. It should be emphasized that the velocity in terms of the slow time variable τ is not zero.

The eigenvalues, λ , of the Jacobian of f satisfy the characteristic polynomial:

$$\lambda^2 + \lambda \left(\left. \frac{\partial a}{\partial z_1} \right|_{z^*} + d \right) + \left(\left. \frac{\partial a}{\partial z_2} \right|_{z^*} + c \right) = 0.\tag{11}$$

200

201

202

203

204

205

The system is unstable when a positive eigenvalue exists and stable when all the eigenvalues are negative. Therefore, if for any τ , exists $z^* = (0, r^*)$, such that $\left. \frac{\partial a}{\partial z_2} \right|_{z^*} + c < 0$ or $\left. \frac{\partial a}{\partial z_1} \right|_{z^*} + d < 0$, the system is unstable. The system is asymptotically stable when $\left. \frac{\partial a}{\partial z_2} \right|_{z^*} + c > 0$ and $\left. \frac{\partial a}{\partial z_1} \right|_{z^*} + d > 0$. The limiting case $\left. \frac{\partial a}{\partial z_2} \right|_{z^*} + c = 0$ or $\left. \frac{\partial a}{\partial z_1} \right|_{z^*} + d = 0$ is of no particular interest for the physical problem at hand and it is not studied herein. However, we can show that in this particular case the system is stable.

The time evolution of the stable solution of the system is $y_0 = y_0^* = y_0^*(\tau)$. We call here this state *steady-state*, given that $\frac{\partial y_0^*}{\partial t} = 0$. Eq.(8).2 becomes:

$$\frac{\partial^2 y_1}{\partial t^2} = -\alpha y_1 - \beta \frac{\partial y_1}{\partial t} - \beta \frac{\partial y_0^*}{\partial \tau} + d,\tag{12}$$

where $\alpha = \left. \frac{\partial a}{\partial y} \right|_{(y_0^*, 0)} + c$, $\beta = \left. \frac{\partial a}{\partial y} \right|_{(y_0^*, 0)} + d$ and $\frac{\partial y_0^*}{\partial \tau}$ can be determined by differentiating Eq.(10.1) in terms of τ :

$$\frac{\partial y_0^*}{\partial \tau} = \frac{c}{\left. \frac{\partial a}{\partial y} \right|_{(y_0^*, 0)} + c} = \frac{c}{\alpha}.\tag{13}$$

The general solution of (12) is:

$$y_1^*(t, \tau) = \frac{\alpha d - \beta c}{\alpha^2} + C_1 e^{\frac{1}{2}(-\beta + \sqrt{\Delta})t} + C_2 e^{\frac{1}{2}(-\beta - \sqrt{\Delta})t}, \quad (14)$$

206 where C_1 and C_2 are constants determined by the initial conditions of the ε^1 problem
 207 and $\Delta = \beta^2 - 4\alpha$.

The asymptotic approximation of the steady-state solution of the problem, y^* , is therefore:

$$y^*(t) = y_0^*(\varepsilon t) + \varepsilon y_1^*(t, \varepsilon t) + O(\varepsilon^2). \quad (15)$$

The steady state velocity, $v^*(t)$, is approximated by the series (see Eq.(5)):

$$v^*(t) = \varepsilon \left[\frac{c}{\alpha} + C_1 \frac{1}{2} (-\beta + \sqrt{\Delta}) e^{\frac{1}{2}(-\beta + \sqrt{\Delta})t} + C_2 \frac{1}{2} (-\beta - \sqrt{\Delta}) e^{\frac{1}{2}(-\beta - \sqrt{\Delta})t} \right] + O(\varepsilon^2). \quad (16)$$

208 Notice that if $\beta > 0$, $v^*(t)$ approximates asymptotically the solution $v^*(t) = \varepsilon \frac{c}{\alpha} +$
 209 $O(\varepsilon^2)$. Positive β is usually the case, due to the high viscosity of the surrounding to the
 210 fault rocks.

2.3 Conditions for steady-state slip of the spring-slider analog

211 Considering a monotonous motion ($\dot{\delta} \geq 0$) of the spring-slider system, the friction can be considered as a non-linear function of slip δ and can be expanded in power series as done in Eq.(7). Under these assumptions, the multiscale asymptotic approach presented above can be used for the spring-slider system. More specifically, according to Eq.(16), the slip-rate at steady-state of the spring-slider model is given by:

$$v_{ss} = \frac{v_\infty}{1 + \frac{1}{k} \frac{\partial F}{\partial \delta}}, \quad (17)$$

where $\frac{\partial F}{\partial \delta}$ is calculated at a given $\delta(t) = \delta_0$ and at zero slip-rate $\dot{\delta} = 0$. The above relation can give a useful global estimation of velocity, if the frictional properties of the system are known. Inversely, if the time evolution of the block velocity is known (e.g. measured), $\frac{\partial F}{\partial \delta}$ can be determined:

$$\frac{\partial F}{\partial \delta} = k \left(\frac{v_\infty}{v_{ss}} - 1 \right). \quad (18)$$

According to the previous paragraph, the steady-state slip is *unstable*, if and only if for any δ_0 :

$$\left. \frac{\partial F}{\partial \delta} \right|_{(\delta_0, 0)} < -k \quad \text{or} \quad \left. \frac{\partial F}{\partial \dot{\delta}} \right|_{(\delta_0, 0)} < -\eta. \quad (19)$$

212 The first condition refers to slip-weakening and coincides with the one described in Di-
 213 eterich (1978) (see also Goodman (1989); Scholz (2002)). The so-called *nucleation length*
 214 (Andrews, 1976) can be retrieved setting $k = A \frac{2}{\pi} \frac{\lambda + \mu}{\lambda + 2\mu} \frac{\mu}{L}$, where λ and $\mu = G$ are the
 215 Lamé constants (μ not to be confused with the friction coefficient in the next paragraphs)
 216 and A the slip area. The second condition shows that the system is unstable when the
 217 friction is slip-rate weakening (velocity-weakening). However, for common parameters
 218 of frictional velocity weakening (Reches & Lockner, 2010) and viscosity of rocks (Vutukuri
 219 & Katsuyama, 1994) this instability condition is not critical.

220 We assume Coulomb friction, $F = \mu N'$, where N' is the effective normal force ap-
 221 plied on the block, as shown in Figure 1, and μ is the friction coefficient. The coefficient
 222 of friction varies from an initial value μ_{\max} (static friction coefficient), to a residual one
 223 μ_{res} (kinetic friction coefficient). Figure 2a shows schematically the transition between
 224 static and kinetic friction. This transition is made in a characteristic distance D_c and
 depends on the frictional properties of the fault system. In Figure 2b we show the in-

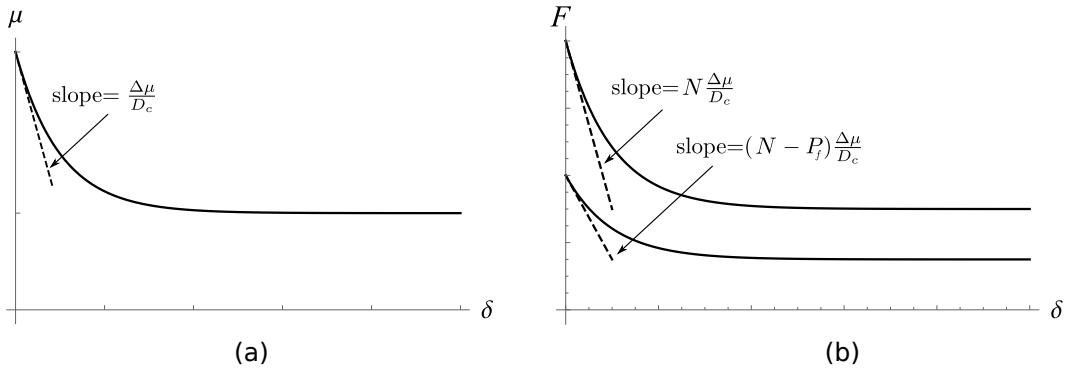


Figure 2. Schematic representation of the evolution with slip of (a) the friction coefficient and (b) of the Coulomb friction force with and without fluid pressure, P_f . The system becomes more ductile (lower slope) when the fluid pressure increases.

225
 226 fluence of N' on the friction force. Due to fluid injection, $N' = N - P_f$, where P_f is
 227 the force exerted to the block by the fluid due to fluid pressure and N the total force which
 228 is a fraction of the overburden load depending on the tectonic setting. Forces can be ex-
 229 pressed in terms of stresses by dividing by the slip area A . It is worth noticing that the
 230 system becomes more ductile for increasing pore pressure due to the dependence of the
 231 slope of the softening branch $(N - P_f) \frac{\Delta \mu}{D_c}$ on P_f , i.e. $(N - P_f)$ multiplies μ . Under con-
 232 stant P_f , unstable, seismic slip happens when $(N - P_f) \frac{\Delta \mu}{D_c} < -k$, provided that the

233 applied destabilizing force from the spring is high enough. If the force exerted from the
 234 spring to the block, $F_s = k(v_\infty - v_{ss})$ is not high enough ($F_s < F$), then no sliding
 235 takes place and the system is stable. Therefore, the necessary condition for instability
 236 is $F_s = F$. In this case we say that an (existing) fault is (re)activated. However, it is
 237 worth emphasizing that this condition is not a sufficient one for seismic slip (unstable
 238 behavior). If the aforementioned instability conditions (19) are not satisfied, we have slip,
 239 but this a slow, aseismic, creep-like slip with velocity given by Eq.(18).

240 From the physical point of view, a dynamic instability takes place if the slip weak-
 241 ening is higher than the negative slope of the effective elastic response of the surround-
 242 ing to the fault rocks or, in other words, when the elastic unloading of the surrounding
 243 rocks cannot be counterbalanced by fault friction. The same happens also when the fric-
 244 tion shows velocity weakening that cannot be counterbalanced by the viscosity of the sur-
 245 rounding rock mass. However, the situation changes when the fluid pressure is not con-
 246 stant with time $P_f = P_f(t)$. The question addressed in the next section is exactly how
 247 one should control $P_f(t)$ in order to assure stable slip.

248 **3 Controlling instabilities**

249 **3.1 Control system configuration**

250 We assume a general negative-feedback control system as depicted in Figure 3. $\Sigma(P)$
 251 is the system to be controlled, the spring-slider in our case, $\Sigma(C)$ the controller we need
 252 to design, $y(t)$, the output of the controlled system $\Sigma(P, C)$, i.e. the displacement of the
 253 block $\delta(t)$, $u(t)$ the input of $\Sigma(P)$, $u_c(t)$ the input of the controller $\Sigma(C)$ and $y_c(t)$ its
 254 output. $u_1(t)$ and $u_2(t)$ are inputs to the system (e.g fluid pressure, long and short range
 255 perturbations, applied slip velocity etc.). We seek the controller $\Sigma(C)$ that can stabi-
 256 lize the spring-slider model by modifying (controlling) the applied fluid pressure $P_f(t)$
 257 (input). The problem is challenging due to friction and the consequent non-linearities
 258 it introduces. Additionally, the pore pressure multiplies the friction coefficient and does
 259 not allow us to write the mathematical system in canonical forms frequently used in the
 260 mathematical theory of control (Vardoulakis, 1991, 2012). However, the target of the present
 261 work is to stabilize the system and stay in the vicinity of an evolving steady-state. This
 262 justifies the linearization of the equations in terms of slip, slip-rate and fluid pressure.

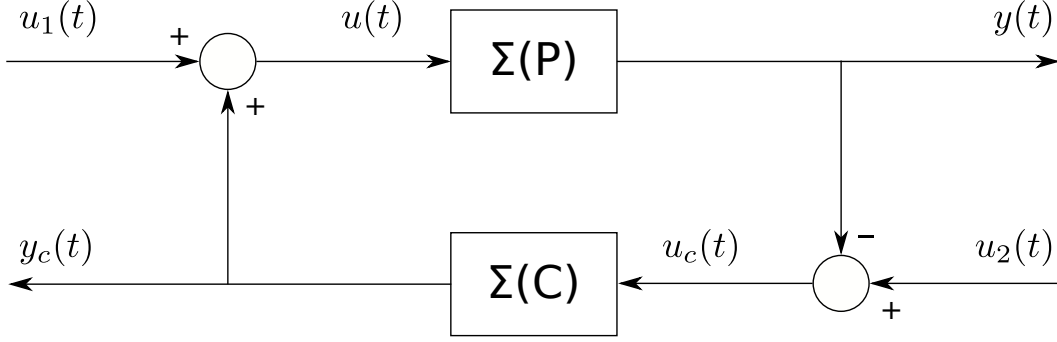


Figure 3. Negative feedback control system $\Sigma(P, C)$. $\Sigma(P)$ is the system to be controlled with the controller $\Sigma(C)$.

263

3.2 Linearization

We want to stabilize the fast dynamics of the system described by Eq.(2). Therefore, we need to assure that the system is stable in the fast time scale described by the order ε^0 in the cascade system of equations (8). Setting $y_0 = \tilde{y} + y_0^*$ in Eq.(8).1 and the same equation expressed at the reference state y_0^* , we obtain:

$$\ddot{\tilde{y}} = -a(\tilde{y} + y_0^*, \dot{\tilde{y}}, \phi) + a(y_0^*, 0, \phi_0^*) - c\tilde{y} - d\dot{\tilde{y}}, \quad (20)$$

where \tilde{y} represents a perturbation of the reference steady-state solution, $\phi = \phi(t)$ the dependence of the $a(y, \dot{y}, \phi)$ function in terms of an input (here the fluid pressure), $\phi(t)$, which takes the reference value ϕ_0^* at steady state. Expanding $a(\tilde{y} + y_0^*, \dot{\tilde{y}}, \phi)$ in power series around $\tilde{y} = 0$, $\dot{\tilde{y}} = 0$ and $\phi = \phi_0^*$ (steady-state) we obtain:

$$\ddot{\tilde{y}} + a_1\dot{\tilde{y}} + a_0\tilde{y} = b_0u, \quad (21)$$

264 where $u(t) = \phi(t) - \phi_0^*$, $a_0 = \alpha = \left. \frac{\partial a}{\partial y} \right|_{(y_0^*, 0, \phi_0^*)} + c$, $a_1 = \beta = \left. \frac{\partial a}{\partial \dot{y}} \right|_{(y_0^*, 0, \phi_0^*)} + d$ and $b_0 =$
 265 $-\left. \frac{\partial \alpha}{\partial \phi} \right|_{(y_0^*, 0, \phi_0^*)}$. In the following, the tilde over y is dropped for simplicity in notation.

266

3.3 Stabilizability

The above equation describes the behavior of the system for small perturbations from its steady-state. It is linear both in terms of y and the input u and its characteristic polynomial is:

$$D(s) = s^2 + a_1s + a_0, \quad (22)$$

while for the input (right-hand-side) is:

$$N(s) = b_0. \quad (23)$$

The transfer function of the system is:

$$P(s) = \frac{N(s)}{D(s)} = \frac{b_0}{s^2 + a_1s + a_0}. \quad (24)$$

267 The poles of the system are at s_0 satisfying $D(s_0) = 0$. As expected, the poles have non-
 268 negative real part when α or β are negative (instability). Since the system has no de-
 269 coupling zeros in the closed right half complex plane, i.e. in $\overline{\mathbb{C}^+} = \{s \in \mathbb{C}, \text{Re}(s) \geq$
 270 $0\}$, the system is *stabilizable*. Decoupling zeros are called the common roots of $N(s)$ and
 271 $D(s)$ that are not roots of its transfer function $P(s)$. Consequently, a stabilizing com-
 272 pensator (stabilizing controller) can be designed. This is a major result for the appli-
 273 cation at hand as it shows that earthquakes can be controlled, at least from the math-
 274 ematical point of view.

275 3.4 Proper stabilizing controller

According to Vardulakis (1991) the system $\Sigma(C)$, with transfer function $C(s) = \frac{Y(s)}{X(s)} \in \mathbb{R}_{pr}(s)$, is a stabilizing compensator, if and only if, the characteristic polynomial of the closed system $\Sigma(P, C)$:

$$D_c(s) = X(s)D(s) + Y(s)N(s), \quad (25)$$

has all its roots in $\mathbb{C}^- = \{s \in \mathbb{C}, \text{Re}(s) < 0\}$. Following the procedure described in Vardulakis (1991, 2012) it is possible to determine $Y(s)$ and $X(s)$ and, therefore, design the desired stabilizing controller. Let $\Lambda_5 = \{\lambda_1, \lambda_2, \lambda_3, \lambda_4, \lambda_5\}$ the set of roots of $D_c(s)$ such that $\lambda_i = \lambda \in \mathbb{C}^-$. The polynomials $X(s)$ and $Y(s)$ are determined by solving the following linear system:

$$\underline{\omega}^T \underline{M}_4 = \underline{d}^T, \quad (26)$$

where \underline{M}_4 is the Wolovich resultant of rank 6 (Antoniou & Vardulakis, 2005):

$$M_4 = \begin{bmatrix} a_0 & a_1 & 1 & 0 & 0 & 0 \\ b_0 & 0 & 0 & 0 & 0 & 0 \\ 0 & a_0 & a_1 & 1 & 0 & 0 \\ 0 & b_0 & 0 & 0 & 0 & 0 \\ 0 & 0 & a_0 & a_1 & 1 & 0 \\ 0 & 0 & b_0 & 0 & 0 & 0 \\ 0 & 0 & 0 & a_0 & a_1 & 1 \\ 0 & 0 & 0 & b_0 & 0 & 0 \end{bmatrix} \quad (27)$$

and

$$\underline{d}^T = \begin{bmatrix} -\lambda^5 & 5\lambda^4 & -10\lambda^3 & 10\lambda^2 & -5\lambda & 1 \end{bmatrix} \quad (28)$$

ω^T contains the coefficients of $X(s)$ and $Y(s)$:

$$\omega^T = \left[\begin{bmatrix} \chi_0 & \psi_0 \end{bmatrix} \begin{bmatrix} \chi_1 & \psi_1 \end{bmatrix} \begin{bmatrix} \chi_2 & \psi_2 \end{bmatrix} \begin{bmatrix} \chi_3 & \psi_3 \end{bmatrix} \right] \quad (29)$$

such that:

$$X(s) = \chi_3 s^3 + \chi_2 s^2 + \chi_1 s + \chi_0 \quad \text{and} \quad Y(s) = \psi_3 s^3 + \psi_2 s^2 + \psi_1 s + \psi_0. \quad (30)$$

The transfer function of the closed system $\Sigma(P, C)$ is then:

$$H_{cl}(s) = \begin{bmatrix} \frac{P(s)}{1+C(s)P(s)} & \frac{P(s)C(s)}{1+C(s)P(s)} \\ -\frac{C(s)P(s)}{1+C(s)P(s)} & \frac{C(s)}{1+C(s)P(s)} \end{bmatrix} \quad (31)$$

and therefore the Laplace transform of the output of the closed system is:

$$\begin{bmatrix} Y(s) \\ Y_c(s) \end{bmatrix} = H_{cl}(s) \begin{bmatrix} U_1(s) \\ U_2(s) \end{bmatrix}, \quad (32)$$

276 where $U_1(s)$ and $U_2(s)$ are the Laplace transforms of the inputs $u_1(t)$ and $u_2(t)$, respec-
277 tively (see Figure 3).

278 3.5 Asymptotic tracking

We want to control the response of the system $y(t)$ in order to asymptotically track a reference input $u_2(t)$ as $t \rightarrow \infty$. In other words, we want the error function $u_c(t) = u_2(t) - y(t)$ tend to zero for $t \rightarrow \infty$. Consider the transfer function between the error function $u_c(t)$ and the reference input $u_2(t)$:

$$S(s) = \frac{U_c(s)}{U_2(s)} = \frac{1}{1 + C(s)P(s)} = \frac{X(s)D(s)}{X(s)D(s) + Y(s)N(s)}, \quad (33)$$

where $U_c(s)$ and $U_2(s)$ are respectively the Laplace transforms of $u_c(t)$ and $u_2(t)$. Let $u_2(t)$ be the step function, such that $u_2(t) = K$ for $t \geq 0$ and zero for $t < 0$ or $u_2(t) = Kt$ for $t \geq 0$ and zero for $t < 0$. Then according to Vardulakis (2012), if $\Sigma(P, C)$ is asymptotically stable, then $\lim_{t \rightarrow \infty} u_c(t) = 0$, if and only if, $C(s)$ has a double pole at $s = 0$ or equivalently if and only if $\chi_0 = 0$ and $\chi_1 = 0$. Solving the linear system (26) under these constraints we determine the stabilizing controller, which has the following coefficients:

$$\begin{aligned} \chi_0 = 0, \chi_1 = 0, \chi_2 = -(a_1 + 5\lambda), \chi_3 = 1 \\ \psi_0 = -\frac{\lambda^5}{b_0}, \psi_1 = \frac{5\lambda^4}{b_0}, \psi_2 = \frac{5a_0\lambda + a_0a_1 - 10\lambda^3}{b_0}, \psi_3 = \frac{5a_1\lambda + a_1^2 - a_0 + 10\lambda^2}{b_0} \end{aligned} \quad (34)$$

and therefore:

$$C(s) = \frac{Y(s)}{X(s)} = \frac{\psi_3 s^3 + \psi_2 s^2 + \psi_1 s + \psi_0}{(\chi_3 s + \chi_2) s^2}. \quad (35)$$

279

3.6 Approximate frictional parameters

Knowing a priori the frictional parameters of a fault system is practically impossible. Various geophysical methods can give only approximate estimations. Given a controller designed as described in the previous paragraphs, we will investigate here the tolerance in the frictional parameters that guarantee stabilization. Let $\Sigma(P)$ be the system for which a stabilizing controller, $\Sigma(C)$, was designed and $\Sigma(P')$ the real system that having different frictional parameters than $\Sigma(P)$. The characteristic polynomial of the closed system $\Sigma(P', C)$ is:

$$D'_c(s) = X(s)D'(s) + Y(s)N'(s), \quad (36)$$

Let also the frictional parameters of $\Sigma(P')$ be $a'_0 = a_0 + \Delta a_0 = \left. \frac{\partial a'}{\partial y} \right|_{(y_0^*, 0, \phi_0^*)} + c$, $a'_1 = a_1 + \Delta a_1 = \left. \frac{\partial a'}{\partial y} \right|_{(y_0^*, 0, \phi_0^*)} + d$ and $b'_0 = b_0 - \Delta b_0 = -\left. \frac{\partial \alpha'}{\partial \phi} \right|_{(y_0^*, 0, \phi_0^*)}$. Then Eq.(36) becomes:

$$D'_c(s) = D_c(s) + X(s)\Delta D(s) + Y(s)\Delta N(s), \quad (37)$$

280

281

282

283

284

where $\Delta D(s) = \Delta a_1 s + \Delta a_0$ and $\Delta N(s) = \Delta b_0$. This system is stable when D'_c is a stable polynomial, i.e. when it has all its roots in \mathbb{C}^- . The stability of the polynomial can be explored using the Hurwitz matrix or approximately using asymptotic methods, which gives the required tolerances for Δa_1 , Δa_0 and Δb_0 in function of λ or numerically for a given system.

285

4 Numerical examples

286

4.1 Geological setting and scaling laws

287

288

289

290

291

292

293

294

We consider a fault system at 5km depth. This is a common depth for many energy-related human activities in the earth's crust and in the range of modern drilling technology. At 5km the normal to the fault stress is about $\sigma_n = 100\text{MPa}$ ($\sigma_n = \frac{W}{A}$) and the fluid pressure $p_f = 50\text{MPa}$ ($p_f = \frac{P_f}{A}$), leading to an effective normal stress of $\sigma'_n = \sigma_n - p_f = 50\text{MPa}$. Notice that these values vary considerably with the tectonic configuration, i.e. they depend on whether the fault system is in extensional, compressional or strike-slip setting. The density of the rock is taken equal to $\rho = 2500\text{kg/m}^3$, its apparent shear modulus equal to $G = 30\text{GPa}$ and its apparent viscosity $C = 10^5\text{MPa s}$.

295 Viscosity is not a well constrained quantity. The chosen value is several orders of mag-
 296 nitude lower than the viscosity of rocks at ambient temperature, in order to account for
 297 the earth's crust temperature gradient and the high deviatoric stresses during (pre-)seismic
 298 slip. We refer to Vutukuri and Katsuyama (1994) for experimental results on viscosity
 299 and its dependence on temperature and high stresses.

The shear stress drop caused by an earthquake varies considerably over the rup-
 ture area. This is due to material heterogeneities, fault roughness, geometrical factors,
 multiphysical couplings, locking etc.. Nevertheless, interesting conclusions can be drawn
 if one considers the average shear stress drop over the whole rupture area, $\Delta\tau$. Accord-
 ing to seismological inversions of actual earthquakes, $\Delta\tau$ varies between 0.1 and 10 MPa.
 Here, we take $\Delta\tau = 5\text{MPa}$. It is worth emphasizing that this is a spatial average of the
 shear stress drop over the whole area of the fault and that stress drop can be much higher
 locally. According to Kanamori and Brodsky (2004) the expected (average) slip is:

$$D = \theta^{-1} G^{-1} L \Delta\tau, \quad (38)$$

where θ is a geometric constant of order unity. The seismic moment is defined as $M_0 =$
 GDA , where A is the rupture area, which here is assumed circular, $A \approx L^2$. Consequently:

$$M_0 = \theta^{-1} L^3 \Delta\tau. \quad (39)$$

The seismic magnitude M_w is defined as follows:

$$M_w = \frac{2}{3} \log_{10} M_0 - 6.07 \quad (M_0 \text{ in Nm}) \quad (40)$$

300 From the above scaling equations it is clear that the magnitude of an earthquake is log-
 301 arithmically related to the length of the fault L , or in other words to the size of the fault's
 302 rupture area.

Assuming $\mu_{max} = 0.6$ and $\mu_{res} = 0.5$ such that $\Delta\tau = \sigma'_n \Delta\mu = 5\text{MPa}$ the spring-
 slider model provides useful insights regarding earthquake instability. It models earth-
 quake nucleation and seismic slip in terms of average quantities. However, it ignores the
 spatial rupture process and propagation, which will be studied in details in a future work.
 Based on field measurements, we take $D_c = 10\text{mm}$. Notice that this value is much higher
 than the D_c measured in the laboratory (Kanamori & Brodsky, 2004). Expressing Eq.(1)
 in the form of Eq.(3) we obtain:

$$a = \frac{\sigma'_n}{\rho L} \mu(\delta) \frac{T^2}{D}, \quad c = \frac{G}{\rho L^2} T^2, \quad d = \frac{C}{\rho L^2} T, \quad (41)$$

303 where T and D are, respectively, any reference/characteristic time and length scales lead-
 304 ing to Eq.(2) such that $\varepsilon = \frac{v_{\infty}}{v_{ref}} \ll 1$, with $v_{ref} = \frac{D}{T}$, and $y = \frac{\delta}{D}$. The denominators
 305 ρL and ρL^2 are derived by considering that the mobilized mass, m , is equal to ρL^3 . Re-
 306 garding friction evolution with slip, i.e. $\mu(\delta)$, two cases are explored here. The first one
 307 is a piece-wise linear function of δ and the second the exponential expression $\mu(\delta) = \mu_{res} \left(1 - \frac{\Delta\mu}{\mu_{res}} e^{-\frac{\delta}{D_c}}\right)$
 308 (Figure 2). We neglect velocity weakening as at low slip velocities it is several orders of
 309 magnitude lower (Reches & Lockner, 2010) than the apparent viscosity of the surround-
 310 ing rock and, therefore, it does not influence instability (Eq.(12)). Finally, we assume
 311 a far field tectonic movement of $v_{inf} = 1\text{cm/year}$.

312 In Figure 4 we present the response of the spring-slider for $L = 5\text{km}$. The equa-
 313 tions of the system were integrated using *Wolfram Mathematica 11.2*. According to Eq.(38)
 314 the seismic slip is 0.83m and, as expected, it coincides with the final displacement ob-
 315 tained from the spring-slider model. The seismic moment is $M_0 = 6.25 \times 10^{17}\text{Nm}$, which
 corresponds to an earthquake of magnitude $M_w = 5.8$.

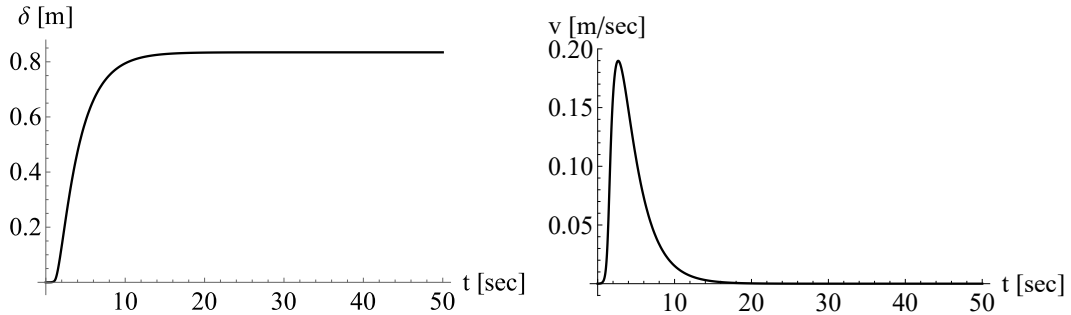


Figure 4. Evolution of slip and slip velocity in function of time for a fault length equal to 5km.

316

317 For smaller fault length $L=500\text{m}$, the seismic moment is $M_0 = 6.25 \times 10^{14}\text{Nm}$
 318 and the magnitude $M_w = 3.8$. Figure 5 shows the evolution of slip and slip-rate for this
 319 fault length as obtained by the spring-slider model. Piece-wise linear or exponential evo-
 320 lution of μ has minor influence on the response of the system.

321 4.2 Scenario #1: Controlling induced seismicity

322 This scenario concerns a fluid injection project in the earth's crust. Examples of
 323 this scenario are deep geothermal projects, deep wastewater disposal, CO_2 sequestra-

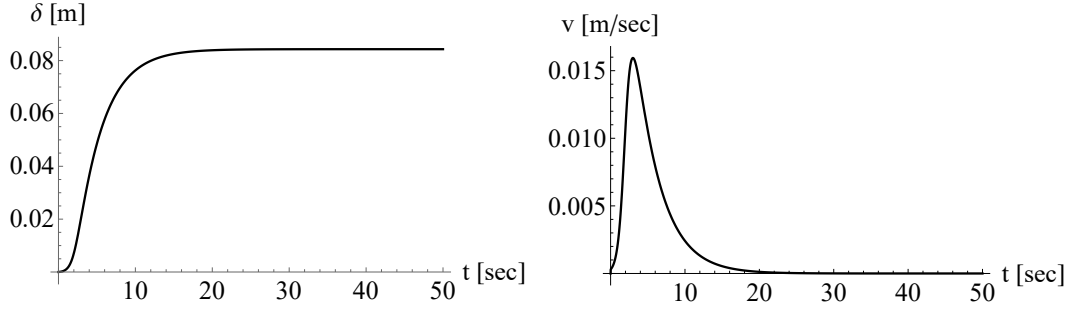


Figure 5. Evolution of slip and slip velocity in function of time for a fault length equal to 500m.

324 tion, unconventional oil and gas production etc. (see Rubinstein and Mahani (2015)).
 325 Of course, in all these projects, avoiding seismic events is of paramount importance. We
 326 assume that the system is not on the verge of instability and that the actual shear stress
 327 due to the far field tectonic movement is lower than the critical one. Critical we call the
 328 average shear stress required to render the system unstable and provoke the earthquake
 329 event of $M_w = 3.8$ described in the previous paragraph (Figure 5). Knowing the ex-
 330 act state of stress in a fault system is not trivial. In this scenario we assume that the real
 331 (average) shear stress state along the fault system of $L=500\text{m}$ is at 90% of the critical
 332 shear stress, i.e. $\tau_{real} = 0.9\tau_{crit}$. At this stress state the system becomes unstable when
 333 the fluid pressure increases for $\Delta p_{f,crit} = 5$ MPa. However, due to inaccurate measure-
 334 ments and other uncertainties, the project coordinators have considered an average shear
 335 stress level lower than the real one. Based on this wrong estimation, they have decided
 336 to inject fluid leading to a maximum fluid pressure increase of $\Delta p_{f,applied} = 10$ MPa,
 337 which is double than $\Delta p_{f,crit}$ and will cause a considerable seismic event without any
 338 control system. The injection program will last one week.

339 To mitigate this risk the fluid pressure increase is continuously regulated by the
 340 stabilizing compensator designed in section 3. We choose $\lambda = -0.1$. The connectivity
 341 of the controller assures negative-feedback to the fault system as shown in Figure 3. We
 342 use the friction parameters at $\delta = 0$ for setting the controller (Eq.(29)). More specif-
 343 ically, $\mu = 0.6$, $\frac{d\mu}{d\delta} = -0.01$ and $a_0 = -3.5 \times 10^{-4}$, $a_1 = 1.6 \times 10^{-1}$, $b_0 = 4.8 \times 10^{-4}$
 344 for $L = 500$ m (see Eq.(41)).

345 Before the reactivation of the fault no slip is observed (locked). Nevertheless, when
 346 the critical fluid pressure is reached the system becomes unstable. The controller suc-

ceeds in stabilizing the system assuring zero slip. No seismicity is observed and the $M_w = 3.8$ earthquake is prevented.

Figure 6 depicts the total pressure change, which is automatically adjusted by the controller. Immediately after fault reactivation, the controller inhibits any further increase of the applied pressure, which according to the injection program should reach 10 MPa. Then it slowly reduces the pressure in order to keep the system stable. This reduction is barely perceptible, but it is necessary for the stabilization of the system. Notice that the far field tectonic velocity is always acting and it has a destabilizing effect as we are at the verge of instability. If the controller is deactivated the system will lose stability and an earthquake of $M_w \approx 3.8$ will take place. In this case we would like to drive safely the system from its unstable state to a stable one. This is the objective of the next paragraph.

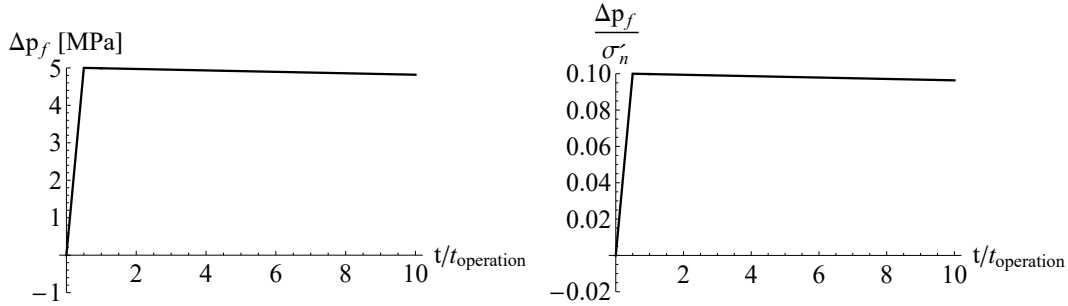


Figure 6. Evolution of fluid pressure change. The total injection operation time was set to 1 week. On the left we present the fluid pressure change and on the right the fluid pressure change normalized by the effective stress at that depth. Immediately after the fault reactivation at $\Delta p_f = 5\text{MPa}$, the controller cancels out the applied pressure and progressively reduces the fluid pressure (suction/pumping) in order to stabilize the system, which is now unstable.

358

359 **4.3 Scenario #2: Controlling earthquakes**

In this paragraph we present an example of active fluid pressure control for avoiding earthquakes, like the ones presented in the previous paragraphs. In particular we focus on avoiding the $M_w = 5.8$ earthquake described in paragraph 4.1 (Figure 4).

Contrary to the previous scenario, in this scenario we don't want to avoid slip, but to induce it in a controllable way. Our target is to assure slow, aseismic slip such as to

364

365 move the system from its initial unstable state to a stable one. In this way we will dis-
 366 sipate in a controllable manner the energy surplus and we will avoid the sudden energy
 367 release that leads to earthquakes.

368 The earthquake control operation is performed in a time window of ten minutes.
 369 The technological feasibility of such an intervention is not discussed herein. We assume
 370 the worst case scenario, i.e. the system is on the verge of instability. However, it is con-
 371 stantly controlled by the stabilizing compensator we designed in Section 3. In this sce-
 372 nario, we choose to make the system slip for 0.83 m, which coincides with the seismic
 373 slip distance of the uncontrolled system (see Figure 4). Consequently, the target veloc-
 374 ity that we want to apply is $v_c \simeq 8.3\text{cm/min}$.

375 As far it concerns the controller, we choose $\lambda = -0.1$ and we calculate its param-
 376 eters using the friction parameters at $\delta = 0$ (Eq.(29)). More specifically, $\mu = 0.6$, $\frac{d\mu}{d\delta} =$
 377 -0.01 and $a_0 = -4.0 \times 10^{-5}$, $a_1 = 1.6 \times 10^{-3}$, $b_0 = 4.8 \times 10^{-5}$ for $L=5\text{km}$ (see
 378 Eq.(41)).

379 In Figure 7 we show the response of the controlled system by integrating the dif-
 380 ferential equations and connecting the controller as shown in Figure 3. We observe that
 381 no abrupt sliding takes place and that the system is successfully controlled (cf. Figure
 382 4). The seismic event is avoided.

383 Figure 8 shows how the controller alters the fluid pressure from its initial hydro-
 384 static value in order to drive the system from its initial unstable state to a stable one
 385 in an aseismic way. We observe that the controller reduces the pressure (pumping, suc-
 386 tion), but in a non-monotonous way. In the beginning of sliding, the fluid pressure is de-
 387 creased rapidly reaching a minimum value of approximately $\Delta p_f = -9$ MPa. This phase
 388 corresponds to the unstable phase of the system (critical distance, D_c). Then the fluid
 389 pressure is progressively increased and when we reach the target distance of the oper-
 390 ation it recovers its initial hydrostatic value, i.e. $\Delta p_f = 0$ MPa. Notice that at this stage,
 391 the fault system is stable even in the absence of the controller ($\frac{d\mu}{d\delta} = 0$, see Eq.(19)).

392 In Figure 9 we compare the kinetic energy of the controlled system with the un-
 393 controlled one. The kinetic energy in the controlled system is four orders of magnitude
 394 lower than the one developed during the seismic event. Moreover, it is practically con-
 395 stant during the earthquake control operation.

396 Figure 10 shows the energy dissipation at the fault. The controlled system dissi-
 397 pates energy under almost constant rate, which depends on the chosen operation time.
 398 Of course, this is not the case for the uncontrolled system where high dissipation rates
 399 are reported due to fast, seismic slip.

400 Finally, Figure 11 illustrates the drop of the elastic energy of the system. Again,
 401 the controlled system manages to reduce its potential energy smoothly (linearly in this
 402 example) and avoid its sudden release as in the case of the uncontrolled system.

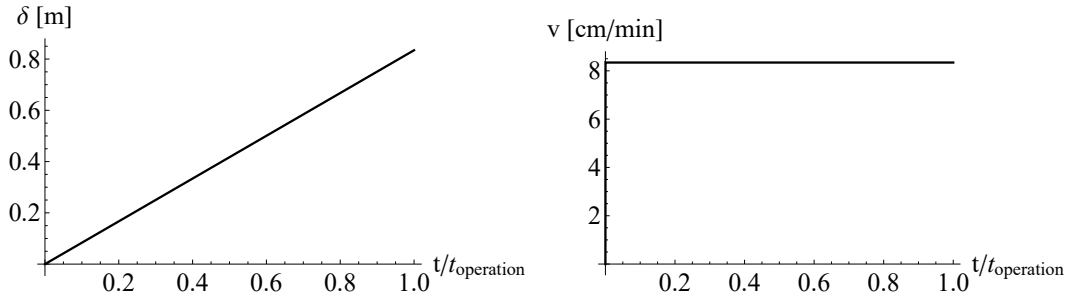


Figure 7. Evolution of slip (left) and slip velocity (right) in function of time normalized with the control operation time (here 10 minutes). The earthquake event is avoided and the system is successfully controlled.

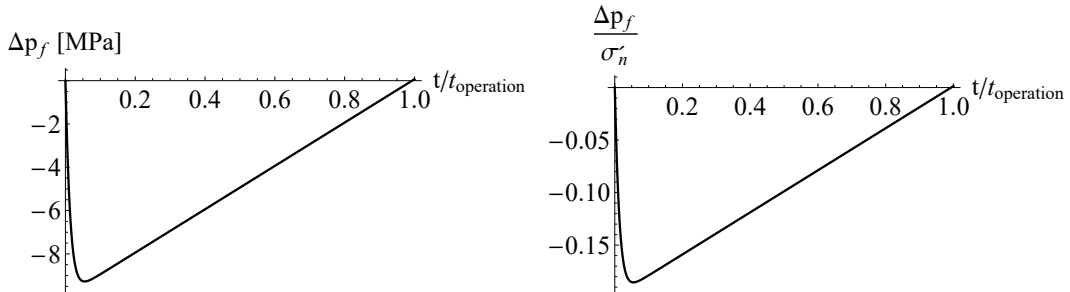


Figure 8. Fluid pressure change, automatically adjusted by the stabilizing controller. On the left we present the fluid pressure change and the on the right the fluid pressure change normalized by the effective stress at that depth. The fluid pressure change is not monotonous and it is calculated in real time by the stabilizing controller.

403 The above simulations were performed with a predetermined friction law that fol-
 404 lows the exponential relation that was given in paragraph 4.1. However, it has to be em-
 405 phasized that the parameters of the controller were kept constant during the simulation
 406 and they were not updated by taking into account the exact evolution of the frictional

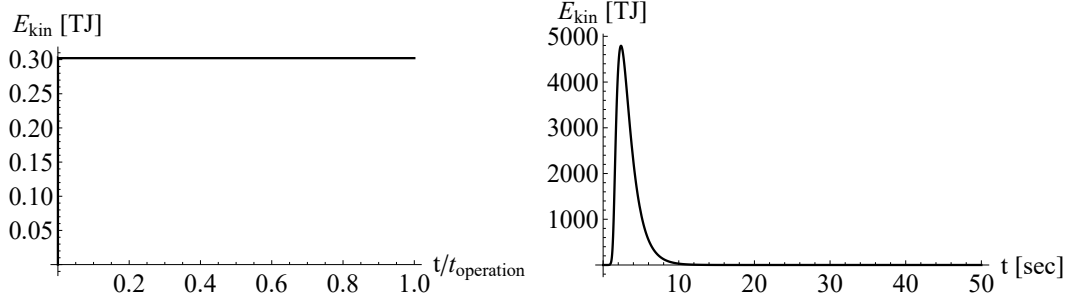


Figure 9. Comparison of the kinetic energy of the controlled system (left) with the uncontrolled one (right). The designed controller manages to reduce four orders of magnitude the kinetic energy and keep it practically constant during the earthquake control operation.

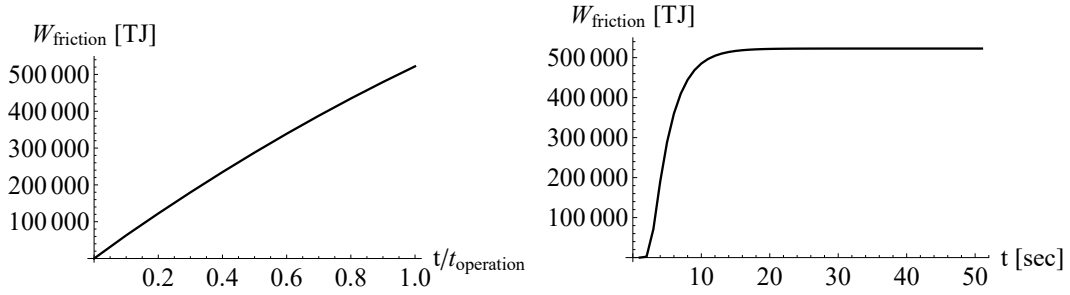


Figure 10. Comparison of energy dissipation due to friction between the controlled system (left) and the uncontrolled one (right). In the controlled system the energy is dissipated progressively, while in the uncontrolled system the energy is dissipated abruptly (earthquake).

407 properties. This shows that the system is controlled even if the frictional properties of
 408 the system are not exactly known (see paragraph 3.6). In order to explore further the
 409 robustness of our approach we keep the same parameters as before for the controller and
 410 we add a sinusoidal perturbation to the friction coefficient as shown in Figure 12. Our
 411 stabilizing controller manages to control the system and avoid the earthquake instabil-
 412 ity despite the fluctuations of the frictional properties. In Figure 13 we show the fluid
 413 pressure change that the controller automatically adjusts to assure stability. The sys-
 414 tem is driven again from its unstable state to a stable one. The perturbation in the fric-
 415 tion coefficient is reflected in the fluctuations of the fluid pressure.

416 5 Conclusions

417 The current paper presents a theoretical work focusing on exploring the possibil-
 418 ity of preventing earthquakes by controlling fluid injection pressure. Our analysis is based
 419 on the classical spring-slider model (frictional slider), which we actively stabilize. We adopt

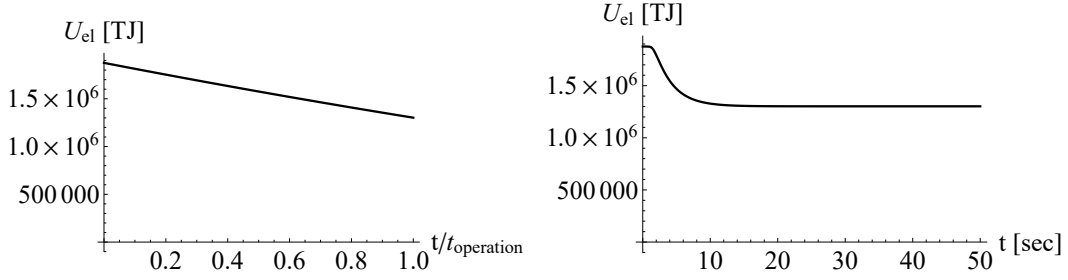


Figure 11. Comparison of the elastic energy drop between the controlled (left) and uncontrolled (right) systems. The designed controller avoids the sudden energy release that happens during an earthquake.

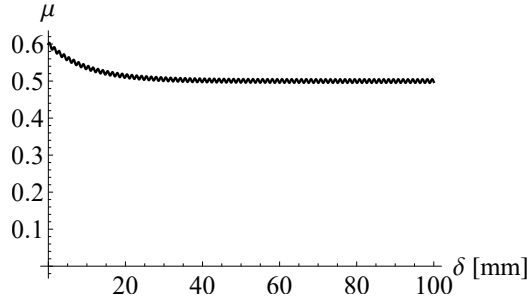


Figure 12. Sinusoidal perturbation of the frictional coefficient.

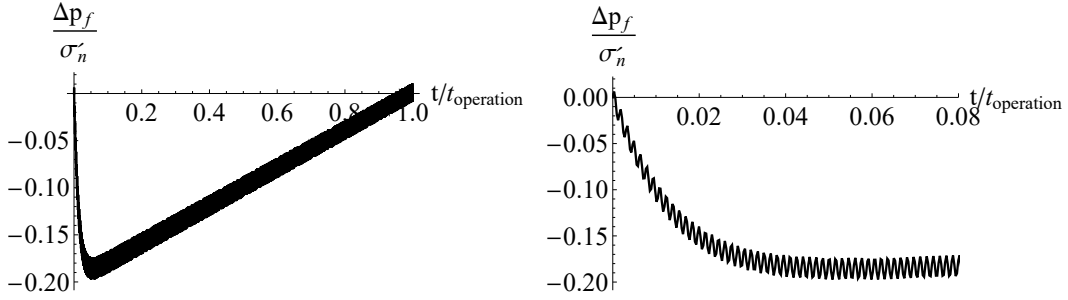


Figure 13. Fluid pressure evolution as calculated by the stabilizing controller for the perturbed friction coefficient (Figure 12). The controller stabilizes the system by automatically adjusting fluid pressure (fluctuations).

420 a general frictional law that accounts for slip and slip rate for the fault behavior. The
 421 fault is considered fully saturated and ideally oriented for slip in the ambient stress-field.
 422 The rocks that surround the fault are considered as a Kelvin-Voigt material.

423 We describe the dynamics of the system using two time scales, i.e. a slow and a
 424 fast one. This scale separation technique allows to asymptotically approximate the so-
 425 lutions of the system as power series of a small parameter, ε , that expresses the ratio be-
 426 tween the fast and the slow time scales. We define as steady-state, the motion that does

427 not involve inertia effects related to the fast time scale at dominant order, ε^0 (Eqs. (8)).
 428 This state represents the slow, creep-like, aseismic motion of the system and has a sim-
 429 ple mathematical expression. More precisely, it is proportional to the far field tectonic
 430 velocity and inversely proportional to a term that involves the first derivative of the ap-
 431 parent friction with respect to slip and the apparent elastic stiffness of the surrounding
 432 the fault rocks (see Eqs.(17) and (18)). The stability of this slow-slip motion is then in-
 433 vestigated using Lyapunov’s first method of stability and the conditions for which steady-
 434 state motion is stable are determined. Notice, that due to the far field tectonic veloc-
 435 ity and the general rheology considered for friction, the system is non-autonomous. With
 436 this double-scale methodology, we manage to alleviate the explicit dependence of the sys-
 437 tem on the fast time scale, rendering it time-invariant at the dominant order.

438 Based on these results and the abovementioned time-invariance, the application of
 439 well established tools of the classical mathematical theory of control is possible. More
 440 specifically, control theory is used for stabilizing the system and make it remain in the
 441 vicinity of an evolving steady-state. This justifies the linearization of the equations in
 442 terms of slip, slip-rate and fluid pressure.

443 We show mathematically that the system is stabilizable by controlling fluid pressure
 444 slip. In other words, it is possible to stabilize and control the system when it is unsta-
 445 ble, by appropriately adjusting the fluid pressure. This is a major result. The contrary
 446 would mean that earthquake control is impossible. Moreover, the opposite conclusion
 447 would imply that ongoing, large-scale industrial applications, involving injection of large
 448 quantities of fluids in the earth’s crust, have high degree of risk, which cannot be mit-
 449 igated.

450 Assuming a general negative-feedback control system, we designed a proper sta-
 451 bilizing controller. By monitoring slip, the designed controller succeeds in adjusting the
 452 fluid pressure and assures stable, aseismic slip, even in the absence of complete knowl-
 453 edge of the exact frictional properties of the system (robustness). Moreover, it succeeds
 454 in automatically controlling the pore fluid pressure and impose a prescribed slip or slip
 455 velocity (asymptotic tracking). These features of the controller allow a) to mitigate the
 456 seismic risk related to induced seismicity and b) to drive the system from an unstable
 457 state of high energy to a stable one of lower energy with constant slip velocity.

458 These features are illustrated through two scenarios of earthquake control. In these
 459 scenarios, fluids are injected under controlled pressure at 5km depth. More specifically,
 460 the first scenario refers to a fictitious injection project, where injection under constant
 461 pressure rate was planned. It is shown that the controller automatically stabilizes the
 462 system and avoids the anticipated earthquake event of $M_w = 3.8$. In particular, the con-
 463 troller inhibits any further fluid pressure increase when the system enters to the unsta-
 464 ble regime. This is done automatically by the controller by simply monitoring slip evo-
 465 lution. In this way the earthquake event is avoided. As the time increases, the controller
 466 progressively reduces the fluid pressure by pumping, in order to prevent seismic slip. Fluid
 467 removal reminds us the hypothetical scheme for EQ control proposed by Raleigh et al.
 468 (1976) and the related experiment at Rangely, Colorado in USA. However, with our ap-
 469 proach, fluid pressure is automatically regulated in real-time, based on a designed negative-
 470 feedback control system. Consequently, more complex situations can be treated and sta-
 471 bility can be actively assured without prescribing the fluid pressure history in advance.

472 The next scenario concerns the mitigation of a $M_w = 5.8$ event by imposing con-
 473 stant slip velocity. For simplicity we assume that we are at the verge of unstable, seis-
 474 mic slip. The controller reduces the fluid pressure by pumping, but this is done in a non-
 475 monotonous way. In the beginning of (imposed, desired) sliding, the fluid pressure is de-
 476 creased rapidly reaching a minimum value of approximately $\Delta p_f = -9$ MPa. This phase
 477 corresponds to the unstable phase of the system (slip smaller than the critical distance,
 478 D_c). Then, the fluid pressure is progressively increased by the controller and, finally, it
 479 recovers its initial hydrostatic value. At this stage, the fault system is stable. During the
 480 controlled injection, the kinetic energy is kept constant and it is four orders of magni-
 481 tude lower than the one that would develop abruptly, if the system was not controlled
 482 (seismic event). Regarding energy dissipation, the controller assures an almost constant
 483 dissipation rate, which depends on the chosen operation time. The same happens with
 484 the elastic energy, which is decreased smoothly over the duration of the EQ control op-
 485 eration. Of course, this is not the case for the uncontrolled system, where high dissipa-
 486 tion rates and fast elastic energy drop are observed due to fast, sudden, seismic slip. No-
 487 tice, that in the case of faults that are not at the verge of instability, the controller would
 488 increase the pore fluid pressure to enhance slip and then, once the system enters to the
 489 unstable regime, it would automatically reduce the pore-fluid pressure in order to sta-
 490 bilize the system and drive it to a stable state of lower energy, as mentioned above.

491 The above two scenarios show the ability of the designed controller to prevent earth-
 492 quake events. Of course, these are academic examples and intensive research is needed
 493 before eventual real-scale applications. Notice that both physics and geometry of the fault
 494 system are kept as simple as possible. The role of heterogeneities, of pore fluid diffusiv-
 495 ity and special hydrological conditions are not considered as well. Moreover, fault rup-
 496 ture and slip propagation is considered only on average over the whole fault's length. The
 497 investigation of the above mentioned limitations, as well as the observability of the real
 498 system and other techno-economical aspects of EQ control, exceed the scope of the present
 499 article and they are explored in the frame of the ongoing ERC project "Controlling earth-
 500 Quakes - CoQuake" (<http://coquake.com>).

501 **Acknowledgments**

502 I would like to thank A.I.Vardoulakis for his insightful reviews and help in control the-
 503 ory.

504 This work was supported by the European Research Council (ERC) under the European
 505 Union Horizon 2020 research and innovation program (Grant agreement no. 757848 Co-
 506 Quake). This paper contains no data.

507 **References**

- 508 Andrews, D. J. (1976, nov). Rupture velocity of plane strain shear cracks. *Jour-*
 509 *nal of Geophysical Research*, 81(32), 5679. Retrieved from [http://doi.wiley](http://doi.wiley.com/10.1029/JB081i032p05679)
 510 [.com/10.1029/JB081i032p05679](http://doi.wiley.com/10.1029/JB081i032p05679) doi: 10.1029/JB081i032p05679
- 511 Anthony, J. L., & Marone, C. (2005). Influence of particle characteristics on granu-
 512 lar friction. *Journal of Geophysical Research: Solid Earth*, 110(8), 1–14. doi:
 513 10.1029/2004JB003399
- 514 Antoniou, E. N., & Vardoulakis, A. I. (2005). On the computation and parametriza-
 515 tion of proper denominator assigning compensators for strictly proper plants.
 516 *IMA Journal of Mathematical Control and Information*, 22(1), 12–25. doi:
 517 10.1093/imamci/dni002
- 518 Bender, C. M., & Orszag, S. a. (1999). *Advanced Mathematical Methods for Scien-*
 519 *tists and Engineers I* (Vol. 63) (No. 424). New York: Springer-Verlag.
- 520 Ben-Zion, Y., & Sammis, C. G. (2003, mar). Characterization of Fault Zones.

- 521 *Pure and Applied Geophysics*, 160(3), 677–715. Retrieved from papers2://
 522 publication/uuid/B5D8E702-ED12-48C9-8586-FCDE3DC3A6Chttp://
 523 link.springer.com/10.1007/PL00012554 doi: 10.1007/PL00012554
- 524 Brantut, N., & Sulem, J. (2012). Strain Localization and Slip Instability in a Strain-
 525 Rate Hardening, Chemically Weakening Material. *Journal of Applied Mechan-*
 526 *ics*, 79(3), 031004. Retrieved from [http://link.aip.org/link/JAMCAV/v79/](http://link.aip.org/link/JAMCAV/v79/i3/p031004/s1)
 527 [i3/p031004/s1](http://link.aip.org/link/JAMCAV/v79/i3/p031004/s1){\&}Agg=doi doi: 10.1115/1.4005880
- 528 Brauer, F., & Nohel, J. (1969). *The Qualitative Theory of Ordinary Differential*
 529 *Equations: An Introduction*. New York: Dover Publications.
- 530 Brodie, K., Fettes, D., Harte, B., & Schmid, R. (2007). *Structural terms including*
 531 *fault rock terms*.
- 532 Burridge, R., & Knopoff, L. (1967). Model and theoretical seismicity. *Bulletin of the*
 533 *Seismological Society of America (1967)*, 57(3), 341–371.
- 534 Cappa, F., Scuderi, M. M., Collettini, C., Guglielmi, Y., & Avouac, J.-P. (2019,
 535 mar). Stabilization of fault slip by fluid injection in the laboratory and
 536 in situ. *Science Advances*, 5(3), eaau4065. Retrieved from [http://](http://advances.sciencemag.org/http://advances.sciencemag.org/lookup/doi/10.1126/sciadv.aau4065)
 537 [advances.sciencemag.org/http://advances.sciencemag.org/lookup/](http://advances.sciencemag.org/http://advances.sciencemag.org/lookup/doi/10.1126/sciadv.aau4065)
 538 [doi/10.1126/sciadv.aau4065](http://advances.sciencemag.org/http://advances.sciencemag.org/lookup/doi/10.1126/sciadv.aau4065) doi: 10.1126/sciadv.aau4065
- 539 Cornet, F. H. (2016). Seismic and aseismic motions generated by fluid injec-
 540 tions. *Geomechanics for Energy and the Environment*, 5, 42–54. Re-
 541 trieved from <http://dx.doi.org/10.1016/j.gete.2015.12.003> doi:
 542 10.1016/j.gete.2015.12.003
- 543 Deichmann, N., & Giardini, D. (2009). Earthquakes Induced by the Stimula-
 544 tion of an Enhanced Geothermal System below Basel (Switzerland). *Seis-*
 545 *mological Research Letters*, 80(5), 784–798. Retrieved from [https://](https://pubs.geoscienceworld.org/srl/article/80/5/784-798/143596)
 546 pubs.geoscienceworld.org/srl/article/80/5/784-798/143596 doi:
 547 10.1785/gssrl.80.5.784
- 548 Dieterich, J. H. (1978). Time-dependent friction and the mechanics of stick-slip.
 549 *Pure and Applied Geophysics*, 116(4-5), 790–806. Retrieved from [http://link](http://link.springer.com/10.1007/BF00876539)
 550 [.springer.com/10.1007/BF00876539](http://link.springer.com/10.1007/BF00876539) doi: 10.1007/BF00876539
- 551 Fletcher, J. B., & Sykes, L. R. (1977, sep). Earthquakes related to hydraulic mining
 552 and natural seismic activity in western New York State. *Journal of Geophys-*
 553 *ical Research*, 82(26), 3767–3780. Retrieved from <http://doi.wiley.com/10>

- 554 .1029/JB082i026p03767 doi: 10.1029/JB082i026p03767
- 555 Frohlich, C. (2012). Two-year survey comparing earthquake activity and injection-
556 well locations in the Barnett Shale, Texas. *Proceedings of the National
557 Academy of Sciences*, *109*(35), 13934–13938. doi: 10.1073/pnas.1207728109
- 558 Goodman, R. E. (1989). *Introduction to Rock Mechanics*. John Wiley & Sons, Inc.
- 559 Guglielmi, Y., Cappa, F., Avouac, J.-P., Henry, P., & Elsworth, D. (2015, jun). Seis-
560 micity triggered by fluid injection-induced aseismic slip. *Science*, *348*(6240),
561 1224–1226. Retrieved from [http://www.sciencemag.org/cgi/doi/10.1126/
562 science.aab0476](http://www.sciencemag.org/cgi/doi/10.1126/science.aab0476) doi: 10.1126/science.aab0476
- 563 Healy, J. H., Rubey, W. W., Griggs, D. T., & Raleigh, C. B. (1968, sep). The Den-
564 ver Earthquakes. *Science*, *161*(3848), 1301–1310. Retrieved from [http://www
565 .sciencemag.org/cgi/doi/10.1126/science.161.3848.1301](http://www.sciencemag.org/cgi/doi/10.1126/science.161.3848.1301) doi: 10.1126/
566 science.161.3848.1301
- 567 Hubbert, M. K., & Rubey, W. W. (1959). Role of Fluid Pressure in Mechan-
568 ics of Overthrust Faulting. *GSA Bulletin*, *70*(2), 115–166. Retrieved
569 from <http://bulletin.geoscienceworld.org/content/70/2/115> doi:
570 10.1130/0016-7606(1959)70[115:rofpim]2.0.co;2
- 571 Kanamori, H., & Brodsky, E. E. (2004). The physics of earthquakes.
572 *Reports on Progress in Physics*, *67*(8), 1429–1496. Retrieved from
573 [http://stacks.iop.org/0034-4885/67/i=8/a=R03?key=crossref
574 .0eb46da79cd6938ce542994e8554673e](http://stacks.iop.org/0034-4885/67/i=8/a=R03?key=crossref) doi: 10.1088/0034-4885/67/8/R03
- 575 Keranen, K. M., Savage, H. M., Abers, G. A., & Cochran, E. S. (2013). Potentially
576 induced earthquakes in Oklahoma, USA: Links between wastewater injection
577 and the 2011 Mw 5.7 earthquake sequence. *Geology*, *41*(6), 699–702. doi:
578 10.1130/G34045.1
- 579 Lyapunov, A. M. (1892). *The general problem of the stability of motion* (Doctoral
580 Thesis (in Russian)). University of Kharkov.
- 581 McGarr, A. (2014, feb). Maximum magnitude earthquakes induced by fluid injec-
582 tion. *Journal of Geophysical Research: Solid Earth*, *119*(2), 1008–1019. Re-
583 trieved from <http://doi.wiley.com/10.1002/2013JB010597> doi: 10.1002/
584 2013JB010597
- 585 Okubo, K., Bhat, H. S., Rougier, E., Marty, S., Schubnel, A., Lei, Z., ... Klinger,
586 Y. (2019). Dynamics, radiation and overall energy budget of earth-

- 587 quake rupture with coseismic off-fault damage. , 1–41. Retrieved from
588 <http://arxiv.org/abs/1901.01771>
- 589 Palmer, A. C., & Rice, J. R. (1973). The Growth of Slip Surfaces in the Progressive
590 Failure of Over-Consolidated Clay. *Proceedings of the Royal Society A: Mathe-*
591 *matical, Physical and Engineering Sciences*, 332(1591), 527–548.
- 592 Petersen, M., Mueller, C., Moschetti, M., Hoover, S., Rubinstein, J. L., Llenos, A.,
593 ... Anderson, J. (2015). *Incorporating Induced Seismicity in the 2014 United*
594 *States National Seismic Hazard Model—Results of 2014 Workshop and Sensi-*
595 *tivity Studies* (Tech. Rep.). U.S. Geological Survey.
- 596 Raleigh, C. B., Healy, J. H., & Bredehoeft, J. D. (1976). An experiment in earth-
597 quake control at Rangely, Colorado. *Science (New York, N.Y.)*, 191(4233),
598 1230–7. Retrieved from <http://www.ncbi.nlm.nih.gov/pubmed/17737698>
599 doi: 10.1126/science.191.4233.1230
- 600 Rattez, H., Stefanou, I., & Sulem, J. (2018, jun). The importance of Thermo-
601 Hydro-Mechanical couplings and microstructure to strain localization in 3D
602 continua with application to seismic faults. Part I: Theory and linear sta-
603 bility analysis. *Journal of the Mechanics and Physics of Solids*, 115, 54–
604 76. Retrieved from [http://linkinghub.elsevier.com/retrieve/pii/](http://linkinghub.elsevier.com/retrieve/pii/S0022509617309626)
605 [https://linkinghub.elsevier.com/retrieve/pii/](https://linkinghub.elsevier.com/retrieve/pii/S0022509617309626)
606 [S0022509617309626](https://linkinghub.elsevier.com/retrieve/pii/S0022509617309626) doi: 10.1016/j.jmps.2018.03.004
- 607 Rattez, H., Stefanou, I., Sulem, J., Veveakis, E., & Poulet, T. (2018a, jun).
608 The importance of Thermo-Hydro-Mechanical couplings and microstruc-
609 ture to strain localization in 3D continua with application to seismic faults.
610 Part II: Numerical implementation and post-bifurcation analysis. *Jour-*
611 *nal of the Mechanics and Physics of Solids*, 115, 1–29. Retrieved from
612 <http://linkinghub.elsevier.com/retrieve/pii/S0022509617309638>
613 doi: 10.1016/j.jmps.2018.03.003
- 614 Rattez, H., Stefanou, I., Sulem, J., Veveakis, E., & Poulet, T. (2018b, oct). Numer-
615 ical Analysis of Strain Localization in Rocks with Thermo-hydro-mechanical
616 Couplings Using Cosserat Continuum. *Rock Mechanics and Rock Engineering*,
617 51(10), 3295–3311. Retrieved from [http://link.springer.com/10.1007/](http://link.springer.com/10.1007/s00603-018-1529-7)
618 [s00603-018-1529-7](http://link.springer.com/10.1007/s00603-018-1529-7) doi: 10.1007/s00603-018-1529-7
- 619 Reches, Z., & Lockner, D. A. (2010). Fault weakening and earthquake instability by

- 620 powder lubrication. *Nature*, 467(7314), 452–455. Retrieved from <http://dx>
 621 [.doi.org/10.1038/nature09348](http://dx.doi.org/10.1038/nature09348) doi: 10.1038/nature09348
- 622 Reid, H. F. (1910). The Mechanics of the Earthquake, The California Earthquake of
 623 April 18, 1906. In *Report of the state investigation commission* (Vol. 2). Wash-
 624 ington: Carnegie Institution of Washington.
- 625 Rubinstein, J. L., & Mahani, A. B. (2015). Myths and Facts on Wastewater In-
 626 jection, Hydraulic Fracturing, Enhanced Oil Recovery, and Induced Seis-
 627 micity. *Seismological Research Letters*, 86(4), 1060–1067. Retrieved from
 628 <http://sr1.geoscienceworld.org/lookup/doi/10.1785/0220150067> doi:
 629 10.1785/0220150067
- 630 Scholz, C. H. (2002). *The mechanics of earthquakes and faulting* (Second ed.). Cam-
 631 bridge.
- 632 Scuderi, M. M., Collettini, C., & Marone, C. (2017). Frictional stability and earth-
 633 quake triggering during fluid pressure stimulation of an experimental fault.
 634 *Earth and Planetary Science Letters*, 477, 84–96. Retrieved from <http://>
 635 dx.doi.org/10.1016/j.epsl.2017.08.009 doi: 10.1016/j.epsl.2017.08.009
- 636 Stefanou, I., & Alevizos, S. (2016). Fundamentals of bifurcation theory and
 637 stability analysis. In J. Sulem, I. Stefanou, E. Papamichos, & E. Ve-
 638 veakis (Eds.), *Modelling of instabilities and bifurcation in geomechanics,*
 639 *alert geomaterials doctoral school 2016*. Aussois, France. Retrieved from
 640 <https://www.researchgate.net/publication/334164186>
- 641 Tinti, E., Scuderi, M. M., Scognamiglio, L., Di Stefano, G., Marone, C., & Col-
 642 lettini, C. (2016). On the evolution of elastic properties during laboratory
 643 stick-slip experiments spanning the transition from slow slip to dynamic
 644 rupture. *Journal of Geophysical Research: Solid Earth*, 8569–8594. doi:
 645 10.1002/2016JB013545
- 646 Vardoulakis, A. I. (1991). *Linear Multivariable Control: Algebraic Analysis and Syn-*
 647 *thesis Control*. Chichester, New York, Brisbane, Toronto, Singapore: John Wi-
 648 ley & Sons, Inc.
- 649 Vardoulakis, A. I. (2012). *Introduction to the mathematical theory of the theory of sig-*
 650 *nals, systems and control*. Tziola.
- 651 Veveakis, E., Alevizos, S., & Vardoulakis, I. (2010). Chemical reaction capping of
 652 thermal instabilities during shear of frictional faults. *Journal of the Mechanics*

- 653 *and Physics of Solids*, 58(9), 1175–1194. Retrieved from [http://dx.doi.org/](http://dx.doi.org/10.1016/j.jmps.2010.06.010)
654 10.1016/j.jmps.2010.06.010 doi: 10.1016/j.jmps.2010.06.010
- 655 Veveakis, E., Stefanou, I., & Sulem, J. (2013, may). Failure in shear bands for gran-
656 ular materials: thermo-hydro-chemo-mechanical effects. *Géotechnique Letters*,
657 3(April-June), 31–36. Retrieved from [http://www.icevirtuallibrary.com/](http://www.icevirtuallibrary.com/content/article/10.1680/geolett.12.00063)
658 content/article/10.1680/geolett.12.00063 doi: 10.1680/geolett.12
659 .00063
- 660 Vutukuri, V. S., & Katsuyama, K. (1994). *Introduction to Rock Mechanics*. Indus-
661 trial Publishing and Consulting, Inc.
- 662 Wang, J. H. (2017). Multistable slip of a one-degree-of-freedom spring-slider
663 model in the presence of thermal-pressurized slip-weakening friction and
664 viscosity. *Nonlinear Processes in Geophysics*, 24(3), 467–480. doi:
665 10.5194/npg-24-467-2017